Journal of the European Ceramic Society **19** (1999) 1997–2004

PII: S0955-2219(99)00017-5
0955-2219/99/$ - see front matter

Molten Salt Prepared Lead Titanate: Powder Characterization, Sintering and Physical Properties

H. Idrissi,[a]* A. Aboujalil,[b] J. P. Deloume,[b] G. Fantozzi[a] and B. Durand[c]

[a]Groupe d'Etude de Métallurgie Physique et de Physique des Matériaux, URA 341, Institut National Des Sciences Appliquées, Avenue A. Einstein, 69621 Villeurbanne cedex, France
[b]Laboratoire Energétique et Synthése Inorganique, UPRES A 5079, Université Claude Bernard Lyon1, 43 Boulevard du 11 Novembre 1918, 69622 Villeurbanne cedex, France
[c]Laboratoire de Chimie des Matériaux Inorganiques et Energétiques, UPRES A 5070, Université Paul Sabatier, 118 route de Narbonne, 31062 Toulouse cedex 04, France

(Received 6 February 1998; accepted 22 January 1999)

Abstract

Two tetragonal lead titanate powders, prepared by reaction in molten alkali-metal nitrites, are differentiated by their content in sodium. The role of sodium on the crystal lattice, sintering behaviour and physical properties is discussed. Microstructure and ferroelectric wall domains are shown. Curie temperature is determined from internal friction technique; permittivity and electrical losses are estimated from dielectric measurements. © *1999 Elsevier Science Limited. All rights reserved*

Keywords: lead titanate, powders: chemical preparation, sintering, dielectric properties, molten salts.

1 Introduction

Perovskite type lead titanate $PbTiO_3$ is well known as ferroelectric material with high Curie temperature (490°C). It is generally synthesized by solid state reaction, sol-gel process, chemical precipitation, or hydrothermal treatment.[1–4] In all these methods, a calcination at more or less high temperature is needed to get pure crystallized ferroelectric $PbTiO_3$. In contrast to $BaTiO_3$[5] and $SrTiO_3$[6] powders, leading to dense ceramics, pure lead titanate powders often lead to poor densities because of the large tetragonality of crystal lattices ($c/a = 1{\cdot}063$). However, the densities can be improved by addition of a doping element such as Nb, Ta, Ca, Co, Sr, Ba.[7–9]

Nano-sized yttria stabilized zirconia powders were precipitated, a few years ago, by simultaneous reaction of yttrium and zirconium salts in a molten salt medium at about 450°C.[10,11] The powders were characterized by a high specific surface area and a very homogenous chemical composition. Moreover, high densities were achieved by pressureless sintering at temperatures in the range 1500–1600°C, leading to ceramic bodies with satisfying mechanical properties.[12]

The present paper concerns the morphological characterization of powders, the sintering behaviour and the physical properties of two lead titanates samples, precipitated from molten salt reactions, one pure and the other containing sodium.

2 Experimental

The two lead titanate samples were prepared at 500°C for 2 h, by reaction of lead nitrate (Janssen > 99%) and titanium oxychloride $Ti_2O_3Cl_2$ (laboratory prepared) with molten alkali metal nitrites following a procedure previously described elsewhere.[13,14] For the first one named PT1, the molten salt medium was potassium nitrite KNO_2 (Fluka > 98%, mp = 440°C); for the second one named PT2, it was the eutectic between sodium nitrite $NaNO_2$ (Prolabo > 99%) and potassium nitrite KNO_2 (65 mol% $NaNO_2$, mp = 224°C).

The obtained powders were identified by X-ray diffraction (automatic diffractometer for powders Siemens 500, working with Cu K_α radiation). The

*To whom correspondence should be addressed at: Department de Physique, Facultè des Sciences Aïn Chock, Université Hassan II, Casablanca.

mean size of crystallites was evaluated by peak broadening using silica as reference. The refining of lattice parameters was performed from patterns recorded with silicon as internal standard. The morphology was examined by scanning and transmission electron microscopy (Jeol 200 CX and Philips XL 20). The chemical composition was established from element analysis, performed in the CNRS Microanalysis Center of Solaize.

For physical investigations, lead titanate powders were consolidated by uniaxial pressing up to 50 MPa followed by isostatic pressing up to 400 MPa. Then bodies were sintered in PbO saturated atmosphere, in the range 1050–1150°C for 2 h and at a rate of 5°C/min^{-1}. Densities were determined by Arthur's method.[15]

Sintered bodies were characterized by internal friction technique and dielectric measurements. For high frequencies (1 to 2 kHz), mechanical losses Q^{-1} and Young's modulus E were measured as a function of temperature, from samples driven in flexural vibration at resonance frequency. In agreement with Nowick *et al.*[16] Q^{-1} and E were calculated from the resonance curves via relations (1) and (2):

$$Q^{-1} = \Delta fr/fr\sqrt{3} \tag{1}$$

fr is the resonance frequency and Δfr is the width at half maximum

$$E = 0{\cdot}9464\rho l^4 fr^2/d^2 \tag{2}$$

ρ is the density, l the length and d the thickness of the sample.

$Q^{-1}(T)$ and $E(T)$ were recorded under primary vacuum from -160 to 500°C at a rate of 1°C/min. The frequency of vibration was about 2 kHz and the maximum strain amplitude was 10^{-6}.

For low frequencies (< 1 Hz), the shear modulus $G(T)$ and the mechanical losses $Q^{-1}(T)$ were measured using an inverted pendulum with a maximum strain amplitude of 5×10^{-5}. The sample was settled at its extremities and twisted upon around the longitudinal vertical axis. The dynamic modulus was expressed according to relation (3):

$$G^* G\exp(j\phi) = G' + jG'' \tag{3}$$

ϕ is the lag angle between the strain and the stress.

The mechanical losses versus temperature $Q^{-1}(T)$ were given by the ratio G'/G'' and the shear modulus $G(T)$ was equal to G'. Both were measured under vacuum from 25 to 500°C at a heating rate of 1°C/min.

Dielectric measurements were performed, using an H P. impedancemeter at heating rate of about 1°C min, on plate shaped samples ($5\times5\times1$ mm) first polished, then electroded by air dried silver paste. Relative permittivity ε_r and loss factor $\tan\delta$ were given by relations (4) and (5):

$$\varepsilon_r = \varepsilon' - j\varepsilon'' \tag{4}$$

$$\tan\delta = \varepsilon'/\varepsilon'' \tag{5}$$

ε' is the dielectric constant and ε'' the relative loss factor.

3 Powders Characterization

3.1 Powders prepared in molten $NaNO_2$–KNO_2 eutectic, PT2

From thermogravimetric investigations,[13,14] it was shown that the formation of PT2, by reaction in molten $NaNO_2$-KNO_2 eutectic at 500°C for 2 h, proceeds in several steps:

- Formation of TiO_2 before melting
- Lux Flood acido-basic reactions above melting leading to intermediate products, lead oxide PbO and sodium titanates $Na_2Ti_nO_{2n+1}$
- Transformation of intermediate products into $PbTiO_3$.

Lead titanate is obtained as a yellow powder which is identified by XRD, before and after annealing at 1050°C, to the tetragonal variety of $PbTiO_3$ [Fig. 1(a) and (b)]. Compared to the known position of peaks ($PbTiO_3$ macedonite ICDD 6-0452), a shift of experimental peaks is noticed, either towards high angles (001, 101, 111, 002) or towards low angles (100, 110, 200). The refining of lattice parameters leads to $a = 3{\cdot}902\pm 0{\cdot}004$Å, $c = 4{\cdot}086 \pm 0{\cdot}004$Å and $c/a = 1{\cdot}047$. The ratio value is slightly lower than the one commonly found in literature (1·063).[17] It is mainly due to a decrease of parameter c. Calculations were made from the pattern of a PT2 powder annealed at 1050°C with the aim to get a more accurate measurement of peaks positions. However no shift is observed between patterns recorded before and after annealing.

In non annealed $PbTiO_3$, an average crystallite diameter of 65 nm is found from XRD peak [100] broadening. From electron micrographs [SEM and TEM, Fig. 2(a) and (b)] it is shown that lead titanate powders prepared at 500°C are constituted of micron sized aggregates, built by agglomeration of nearly spherical elementary grains. The sizes of the

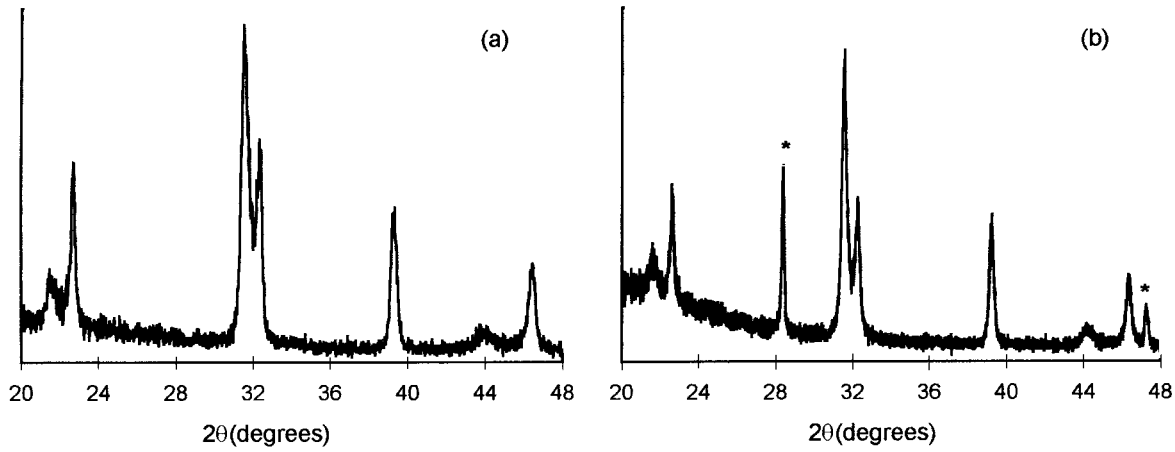

Fig. 1. XRD patterns of $PbTiO_3$ prepared in $NaNO_2$–KNO_2, (a) powder, (b) sintered body, * silicon.

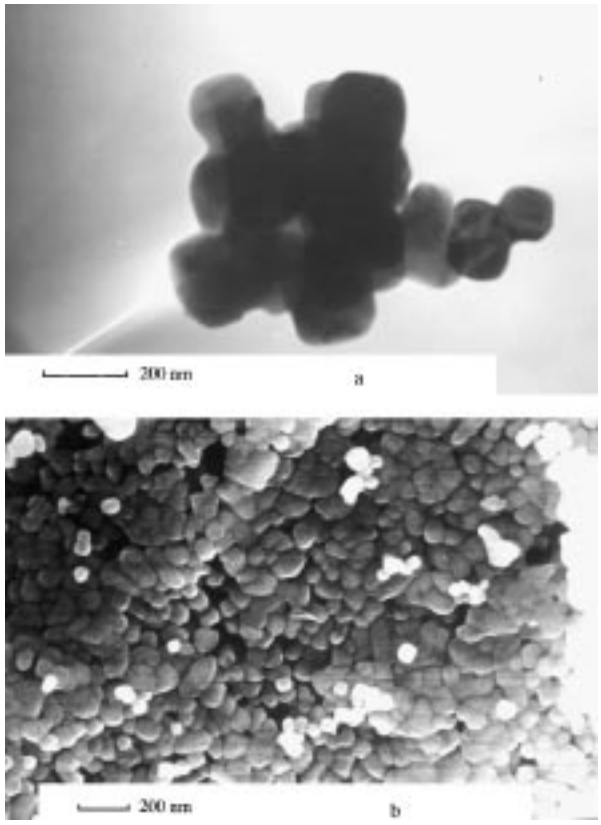

Fig. 2. Micrographs of $PbTiO_3$ powder prepared in $NaNO_2$–KNO_2, (a) TEM, (b) SEM.

latter are in the range 50–150 nm. The agreement with the crystallite size estimated from XRD patterns indicates that elementary grains are monocrystalline. Moreover, a beginning of sintering between crystallites is obviously seen on both kinds of micrographs. This phenomenon is typical of lead titanate powders precipitated from $NaNO_2$–KNO_2 molten medium; it was never observed for instance in zirconia or titania powders prepared in $NaNO_3$–KNO_3 molten medium at similar temperatures.[10,11]

Chemical analysis results of PT2 powder oven dried at 100°C agree with equimolar amounts of lead and titanium and show the presence of a sodium content, higher than the traces of potassium (Table 1) about 10-fold higher if the molar contents are considered. It is noticeable, that sintering at 1050 or 1150°C, carried out by annealing pellets under PbO atmosphere, involves at the same time a decrease of the sodium and potassium contents, probably due to a volatilization of the oxides, and a small decrease of the lead content which can be attributed to the sublimation of the excess of PbO identified in the powders by XRD (Fig. 3).

3.2 Powders prepared in molten KNO_2, PT1

In molten potassium nitrite, the crystallization of PT1, from the same precursors, proceeds also in several steps; however, the formation of potassium titanates is never observed and the only intermediate phases are PbO litharge and TiO_2 anatase.

After aqueous extraction and oven drying at 100°C, the obtained yellow powder is identified by XRD, mainly to the tetragonal variety of $PbTiO_3$ [Fig. 3(a)], besides PbO litharge (ICDD 5-0561) and an unknown phase in small proportion. These latter vanish when the powder is annealed at 1050°C and only tetragonal $PbTiO_3$ remains [Fig. 3(b)]. Compared to $PbTiO_3$ macedonite (ICDD 6-0452), experimental peaks position of PT1 are likewise slightly shifted and the refining of lattice parameters gives $a = 3{\cdot}900 \pm 0{\cdot}004$Å, $c = 4{\cdot}120 \pm 0{\cdot}004$Å and $c/a = 1{\cdot}056$. The value of a is the same as the one obtained for PT2 prepared in $NaNO_2$–KNO_2. The value of c is increased by about 5% The mean size of crystallites estimated from XRD peaks broadening, 50 nm, is of the same magnitude than the one determined for powders prepared in $NaNO_2$–KNO_2. Scanning electron micrographs (Fig. 4) show both large plate shaped agglomerates and smaller particles with sizes in fair agreement with crystallites size.

Chemical analysis data of an oven-dried powder are also in agreement with equimolar amounts of

lead and titanium (Table 1). The content in potassium is higher than in the powders prepared in $NaNO_2$–KNO_2 medium but lower than the content in sodium of these latter.

4 Physical Characterization of Sintered Bodies

Densities achieved by pressureless sintering are 85% of theoretical at 1150°C for PT1 and 95% at 1050°C for PT2. In both cases the chemical composition of the starting powder is not significantly affected by sintering.

4.1 Microstructure and polarization domains

Scanning electron microscopy examination of polished surface submitted to a nitric acid attack shows a mean size of grains of about 3·0 μm for PT1 [Fig. 5(a)] and 2·0 μm for PT2 [Fig. 5(b)]. Polarization domains and domains walls with orientation at 90° and 180° are revealed for both samples.

4.2 Internal friction and elastic modulus

For sample PT1, the Young's modulus versus temperature curve $E(T)$ is characterized by a modulus anomaly A at 480°C, whereas the mechanical losses versus temperature curve $Q^{-1}(T)$ exhibits a high peak P, at the same temperature 480°C and two smaller peaks RI at 380°C and R2 at 310°C (Fig. 6). These curves are recorded at high frequency (< 2 kHz). On the curves $Q^{-1}(T)$ drawn at low frequencies (10^{-2} to 1 Hz) [Fig. 7(a)], it is seen that the temperature of the peak P, 480°C, is independent of frequency, while temperatures of peaks R1 and R2 decrease as the frequency is lowered. As the elastic modulus $E(T)$ at high frequency, the shear modulus versus temperature curves $G(T)$ present at low frequency a modulus anomaly A at 480°C, whatever the frequency [Fig. 7(b)].

The curves of samples PT2, mechanical loss $Q^{-1}(T)$, Young's modulus $E(T)$ at high frequency (Fig. 8) and mechanical loss $Q^{-1}(T)$ [Fig. 9(a)] and shear modulus $G(T)$ [Fig. 9(b)] at low frequencies, are very similar to those of sample PT1. The main difference is a decrease of the temperature of the peak P' and the modulus anomaly A' down to 430°C. On the contrary, the temperatures of peaks R1′ and R2′ are increased respectively to 400 and 360°C. P' and A' are also independent of frequency.

For both samples, the Young's and shear modulus anomalies, A or A', which are associated to the mechanical loss peaks, P or P', correspond to the phase transition tetragonal to cubic which occurs at Curie temperature $Tc = 480$°C for PT1

Table 1. Chemical analysis of lead titanate prepared in the eutectic $NaNO_2$–KNO_2 and in KNO_2 before and after sintering. (Elements contents are given in mass %)

Medium	*$NaNO_2$–KNO_2*		*KNO_2*	
Sample	*Powder*	*Ceramic*	*Powder*	*Ceramic*
Pb	68·5	68·1	68·5	68·2
Ti	15·6	15·8	15.7	15.9
Na	0·6	0·3	—	—
K	0·1	$1{\cdot}5\times10^{-20}$	0·3	0·1
Molar ratio Pb/Ti	1·01	1·00	1·01	0·99

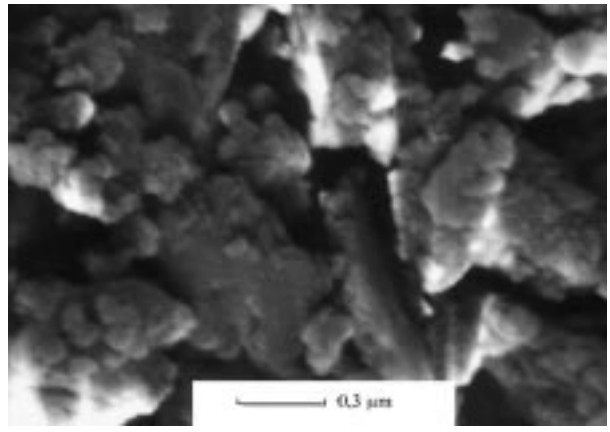

Fig. 4. SEM micrograph of $PbTiO_3$ powder prepared in KNO_2.

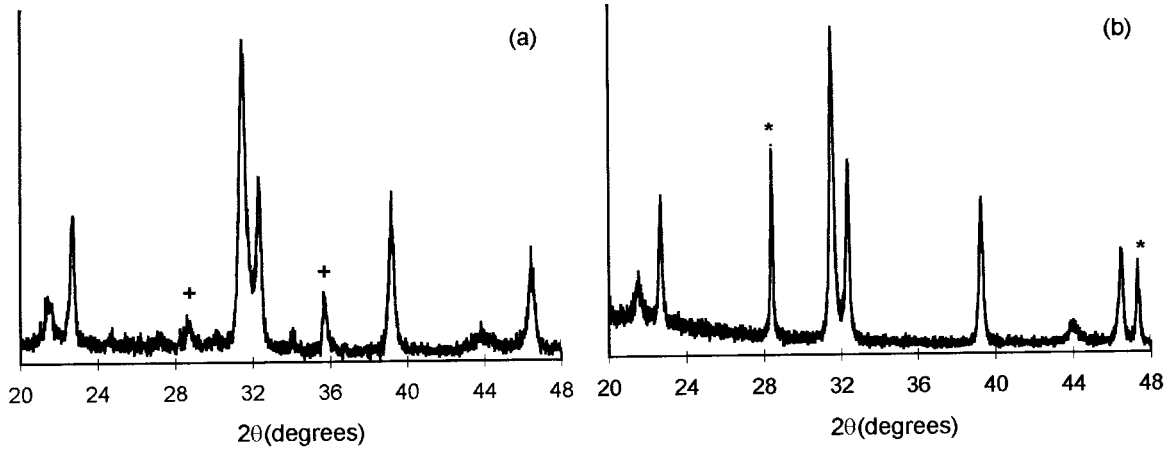

Fig. 3. XRD patterns of $PbTiO_3$ prepared in KNO_2, (a) powder, (b) sintered body. + PbO litharge, * silicon.

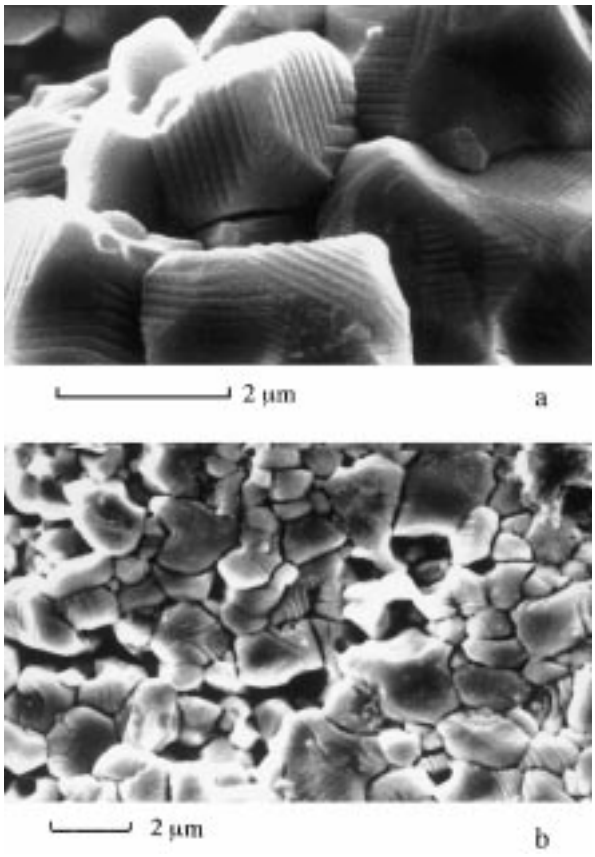

Fig. 5. Microstructure and walls domains, (a) PT1 and (b) PT2.

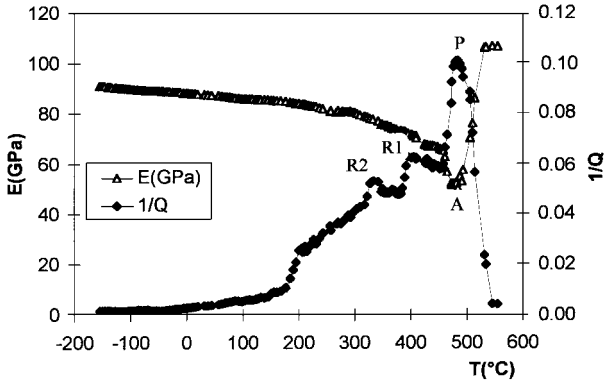

Fig. 6. Young's modulus E and mechanical losses Q^{-1} versus temperature curves recorded for PT1 at high frequency (< 2 kHz).

and $Tc = 430°C$ for PT2. The peaks R of $Q^{-1}(T)$ curves, the temperature of which is dependent of frequency, are attributed to relaxation phenomena.

4.3 Dielectric measurements

Dielectric permittivity ε_r, and losses $\tan\delta$ versus temperature curves are drawn at different frequencies (1, 10, 50 and 100 kHz) for samples PT1 and PT2.

For PT1 (Fig. 10), the permittivity curve exhibits a peak at 480°C, due to the tetragonal–cubic transition. It is all the more distinguished from the

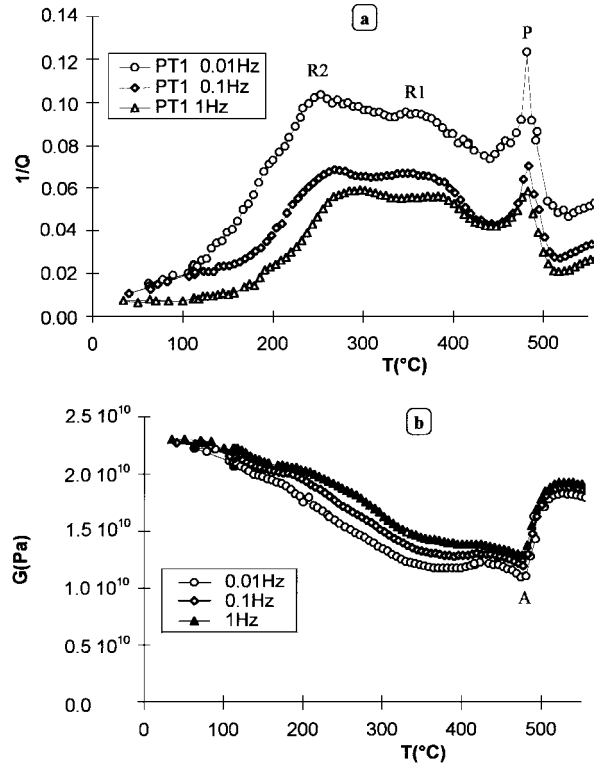

Fig. 7. (a) Mechanical losses Q^{-1} and (b) shear modulus G versus temperature curves recorded for PT1 at different low frequencies.

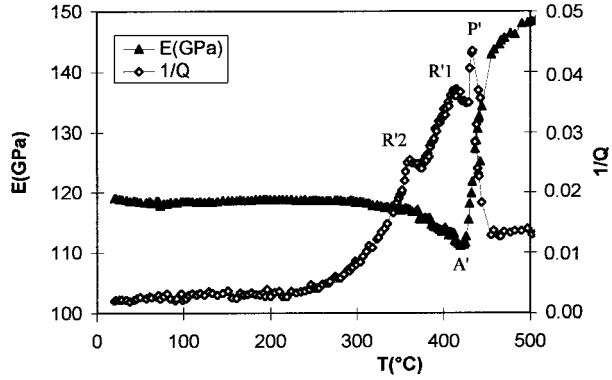

Fig. 8. Young modulus E and mechanical losses Q^{-1} versus temperature curves recorded for PT2 at high frequency (< 2 kHz).

background as the frequency is lowered. Simultaneously the dielectric losses are increased.

For PT2 containing 4 mol% of Na (Fig. 11), the permittivity increases monotonously with the temperature without any transition peak appearance. The dielectric losses are also simultaneously increased. At a given frequency, the dielectric losses are higher for PT2 than for PT1.

5 Discussion

Due to a lower steric hindrance, sodium is liable to enter in the crystal lattice of tetragonal lead titanate at a significantly higher amount than potas-

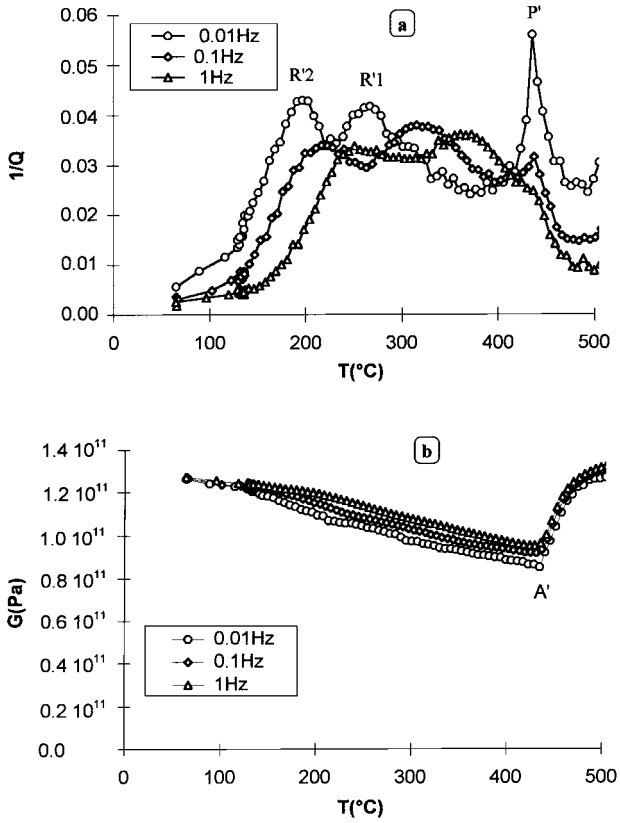

Fig. 9. (a) Mechanical losses Q^{-1} and (b) shear modulus G versus temperature curves recorded for PT2 at different low frequencies.

sium. The presence of sodium simultaneously decreases the tetragonality ($c/a = 1{\cdot}056$ in PT1, 1·047 in PT2). Furthermore, Na-ions replace Pb-ions and O-vacancies are simultaneously created, the valency of sodium being lower than the lead one. So, the O-vacancies diffusion is enhanced during sintering and the sinterability of the PT2 powders is improved in agreement with previous results,[4,7,8] (PT1: $d = 85\%$ at 1150°C, PT2: $d = 95\%$ at 1050°C).

The values of permittivity and dielectric loss at room temperature of the samples PT1 and PT2 are compared in Table 2 to those published for doped $PbTiO_3$[7,18] and pure $BaTiO_3$.[19] Comparing, on the one hand, the samples PT1 and PT2 and, on the other hand, the different doped lead titanates, it is clear that the dielectric constant and losses are dependent upon the nature of the doping element. In the molten salts prepared samples, both are increased by the presence of sodium. For the sodium containing sample PT2, the values of ε_r, and tanδ are similar to those of lead titanate doped with Ni, Fe, Cd or Nb published by Ueda.[18] The absence of peak for the tetragonal–cubic transition, was also observed by the author in $PbTiO_3$ ceramics doped with chromium and partially attributed to an interfacial polarization. The low tanδ value of sample PT1 is of the same magnitude as that of $BaTiO_3$.

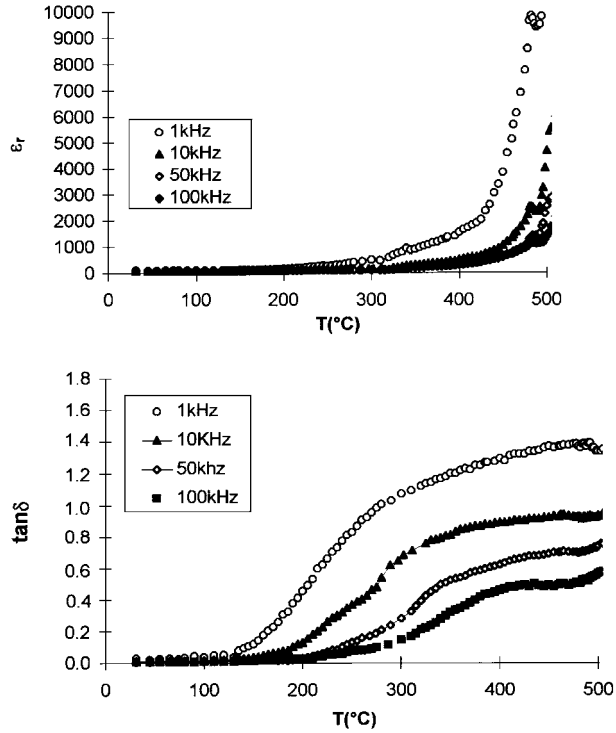

Fig. 10. Dielectric permittivity ε_r, and losses tanδ of PT1 measured at different frequencies.

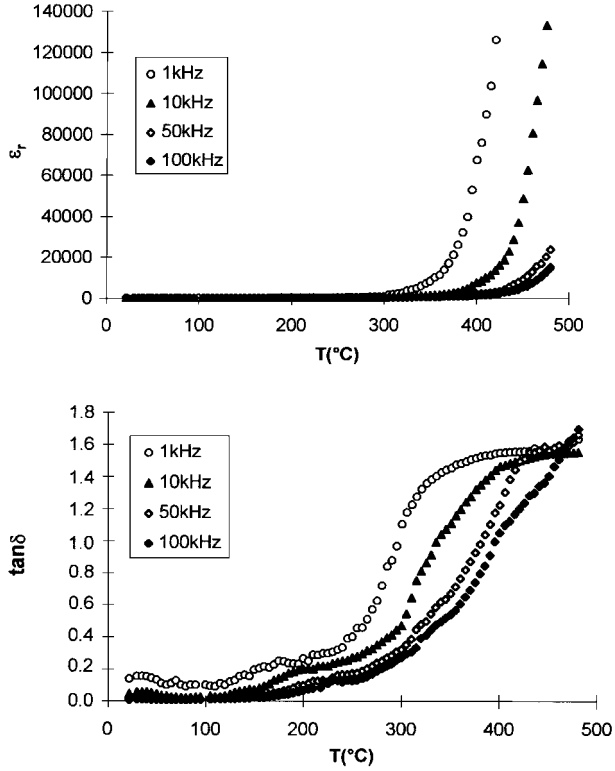

Fig. 11. Dielectric permittivity ε_r and losses tanδ of PT2 measured at different frequencies.

Internal friction versus temperature measurements at different frequencies reveal the phase transition tetragonal–cubic of both samples by a Young's modulus anomaly and a mechanical loss peak. The Curie temperature is localized at 480°C for PT1 and 430°C for PT2. The shift of 50°C

Table 2. Comparison of the experimental values of ε_r, and tanδ of samples PT1 and PT2 with data published in literature for barium titanate and various doped lead titanates

Compound	ε_r	*tan·δ*
$PbTiO_3$ (PT1)	100	0·02
$PbTiO_3$ (PT2)	180	0·13
$PbTiO_3$ + (Ca, Ba, or Sr)	300–600	1·30–2·60
$PbTiO_3$ (Ni, Fe, Nb, Gd, Li, Bi, or Mn)	200	0·01–0·07
$BaTiO_3$	2500	0·03

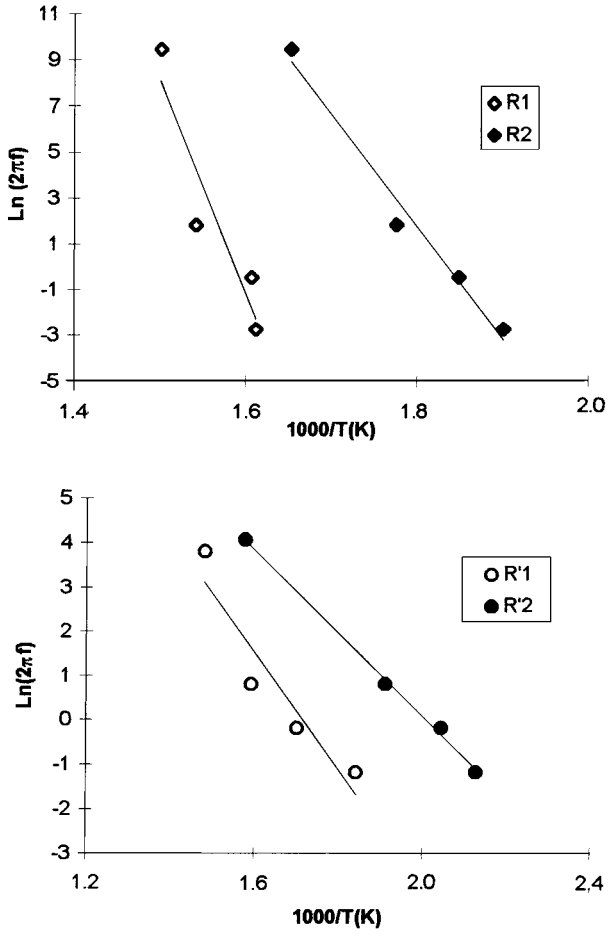

Fig. 12. Arrhenius diagram of peaks R1, R2, R′1, and R′2 for PT1 and PT2.

towards low temperature corroborates the doping effect of sodium. Moreover, measurements carried out at high frequency in the temperature range of −160, 500°C do not show any polymorphic transformation around −100°C for PT1. The existence of such transition in $PbTiO_3$ single crystal was suspected by Kobayashi *et al.*[20] from dielectric measurements, whereas it was set aside by Fontana *et al.*[21] from Raman spectroscopy investigations.

On the mechanical loss curves of PT1 and PT2, the transition peak *P* is preceded by two relaxation peaks R1 and R2. The temperatures of these peaks

Table 3. Activation energy and relaxation time of peaks R

	$PbTiO_3$(PT1)		*$PbTiO_3$(PT2)*	
	R1	*R2*	*R1′*	*R2′*
H (ev)	5·7	2·7	1·6	0·8
$\tau_0(s)$	$1{\cdot}3\times10^{-43}$	$1{\cdot}1\times10^{-27}$	3×10^{-16}	$2{\cdot}7\times10^{-11}$

depend on the vibration frequency. The activation energy (H) and the pre-exponential factor τ_o of these peaks can be calculated using the classical Arrhenius eqn (6).

$$\tau = \tau_0 . \exp(H/kT)$$
$$\tau = \text{relaxation time, k} = \text{Boltzmann constant.} \tag{6}$$

For a Debye peak, the condition for the peak is that ln $(\omega\tau) = 0$. This gives relation (7).

$$\ln(\omega\tau_o) + H/kT_p = 0 \tag{7}$$

where T_p is the peak temperature and $\omega = 2\pi f$ (f is the vibration frequency). The relationship between peak temperatures and vibration frequencies are plotted in Fig. 12 for both samples. From the obtained results (Table 3), it can be noticed that the presence of sodium in lead titanate decreases the activation energy and increases the relaxation time. Similar relaxation peaks were observed in various piezoelectric compounds such as PZT, PHT and $BaTiO_3$.[22–24] They were attributed to movement of domains and to the interaction of oxygen vacancies with domains walls.[24,25] The height of the peak depends on the concentration in oxygen vacancies and on the domain width. In the case of the PT2 lead titanate containing sodium, the grain size is the lowest, but the concentration in oxygen vacancies is the highest. So, the lesser peak heights can be due to a lesser domain width. The relaxation time depends on the oxygen vacancies difflusion. The activation energy obtained for the PT2 specimen is compatible with the activation energy for oxygen vacancies diffusion comparatively with the results obtained for $BaTiO_3$.[24] But, for the PT1 specimen, the values of the activation energy are very high and cannot be linked to a precise mechanism. Further experiments are needed to specify this point.

6 Conclusion

Two lead titanates, were prepared by reaction in molten alkali metal nitrites, the one considered as pure, the other containing 0·3 mass% of sodium. From the investigation of their properties it is

concluded that the insertion of sodium has the following effects:

- The tetragonality of the lattice is decreased by about 1% while the sinterability is improved.
- In both samples, domains are revealed on polished surfaces submitted to a nitric attack, but the Curie temperature is decreased by 50°C. The tetragonal to cubic phase transition is preceded by two relaxation phenomena associated to movement of domains and to diffusion of oxygen vacancies. Activation energy is reduced while relaxation time is increased.

References

1. Ikegami, S., Ueda, I. and Nagta, T., Electromechanical properties of $PbTiO_3$ ceramics containing La and Mn. *J. Acoust. Soc. Am.*, 1971, **50**(4-1), 1060–1066.
2. Blum, G. B. and Gurkovich, S. R., Sol–gel-derived $PbTiO_3$. *J. Mater Scien.*, 1989, **20**, 4479–4483.
3. Safari, A, Lee, Y. H., Halliyal, A. and Newham, R. E, 0–3 piezoelectric composites prepared by coprecipitated $PbTiO_3$ powder. *Am. Ceram. Soc. Bull.*, 1987, **66**(4), 668–670.
4. Takai, K., Shoji, S., Naito, H. and Sawoko, A., In *Proceeding of the First International Symposium on Hydrothermal Reaction*. ed S. Somiya, Gakujustsu and B. Fukya-Kai, Tokyo, Japan, 1982, pp. 877.
5. Cheng, B. L., Gabbay, M. and Fantozzi, G., Anelastic relaxation associated with the motion of domain walls in baryium titanate ceramics. *J. Mat. Sci.*, 1996, **31**, 4141–4147.
6. Poignant, F, L′oxydation de céramiques à base de titanate de strontium semi-conducteur et la formation de barriéres de potentiel aux joints de grains. Ph.D. Thesis no. 21-95, Université de Limoges, Limoges, 1995.
7. Ichinos, N., Yamada, Y., Fuse, Y. and Sato, R., Piezoelectric anisotropy in modified $PbTiO_3$ ceramics. *Jpn. J. App. Phys.*, 1989, **28**(Supp. 28-2), 87–90.
8. Troilo, L. M., Damjanovic, D. and Newnham, R. E., Modified lead calcium titanate ceramics with a relatively large dielectric constant for hydrophone applications. *J. Am. Ceram. Soc.*, 1994, **77**(3), 857–859.
9. Ganesh, R. and Goo, E., Microstructure and dielectric characteristics of $Pb_x(Ba_{0.5}Sr_{0.5})_{(1-x)}TiO_3$ ceramics. *J. Am. Ceram. Soc.*, 1996, **79**(1), 225–232.
10. Jebrouni, M., Durand, B. and Roubin, M., Elaboration de zircone stabilisée á l'yttrium par réaction en milieu nitrate fondu et caractérisation. *Ann. Chim. Science des Matériaux*, 1992, **17**, 143–154.
11. Hamon, D., Vrinat, M., Breysse, M., Jebrouni, M., Durand, B., Roubin, M. and Magnoux, P., Molten salt preparation of stabilized zirconia catalysts: characterization and catalytic properties. *Catalysis Today*, 1991, **10**, 613–627.
12. Jebrouni, M., Préparation de combinaisons á base de zircone par réaction en milieu nitrates fondus. Frittage et propriétés mécaniques. Ph.D. thesis, Université Hassan II, Casablanca, 1996.
13. Aboujalil, A., Synthése en milieu nitrites alcalins fondus de phases ferroélectriques dans les systèmes $BaO–TiO_2$ et $PbTiO_3–PbZrO_3$. Ph.D. thesis no. 212-97, Université C. Bernard Lyon 1, Lyon, 1997.
14. Aboujalil, A., Deloume, J.P., Chassagneux, F., Scharff, J. P. and Durand B., About the reactivity of titanium and lead salts with alkali metal nitrites. *J. Mat. Chem.*, in press.
15. Arthur, G., Porosity and permeability changes during the sintering of copper powder. *J. Inst. Met.*, 1954, **83**, 329–336.
16. Nowick, A. S. and Berry, B. S., Anelastic Relaxation in Crystalline Solids, Academic Press, New York, 1972, Chapter 3.
17. Shirane, G. and Pepinsky, R., X-ray and neutron diffraction study of ferroelectric $PbTiO_3$. *Acta Cryst.*, 1956, **9**, 131–140.
18. Ueda, I., Effects of additives on piezoelectric and related properties of $PbTiO_3$ ceramics. *Jap. J. App. Phys.*, 1972, **11**(4), 450–462.
19. Arlt, G., The influence of microstructure on the properties of ferroelectric ceramics. *Ferroelectrics*, 1990, **104**, 217–227.
20. Kobayashi, J. and Ueda, R., *Phys. Rev. B*, 1956, **103**, 803–805.
21. Fontana, M. D., Idrissi, H. and Kugel, G. R, New Raman results in $PbTiO_3$. *Ferroelectrics*, 1988, **80**, 117–120.
22. Bourim, E. M., Idrissi, H., Cheng, B. L., Gabbay, M. and Fantozzi, G., Elastic modulus and mechanical loss associated with phase transition and domain wall motions in PZT based ceramics. *Journal of Physics*, in press.
23. Idrissi, H., Favotto, C., Roubin, M. and Fantozzi, G., Elaboration and characterization of PHT based ceramics. *Journal of European Ceramic Society*, in press.
24. Cheng, B. L., Etudes des transitions de phase et des mouvements de paroi de domaines, dans les céramiques á base de $BaTiO_3$ par mesures de module élastique et des pertes mécaniques. Ph.D. thesis, INSA-Lyon,1996.
25. Postnikov, V. S., Parlov, V. S., Gridner, S. A. and Turkov, S. K., Interaction between 90° domain walls and point defects of the crystal lattice in ferroelectric ceramics. *Soviet Physics–Solid State*, 1968, **10**(6), 1267–1270.